Available online at www.sciencedirect.com
SCIENCE DIRECT®
Journal of Magnetic Resonance 168 (2004) 1–7
JMR Journal of Magnetic Resonance
www.elsevier.com/locate/jmr

Chemically amplified ^{19}F–^{1}H nuclear Overhauser effects

I. Kuprov and P.J. Hore*

Department of Chemistry, University of Oxford, Physical and Theoretical Chemistry Laboratory, South Parks Road, Oxford OX1 3QZ, UK

Received 5 November 2003

Abstract

Chemically induced dynamic nuclear polarisation (CIDNP) is explored as a source of nuclear hyperpolarisation in heteronuclear Overhauser effect experiments. A photochemical reaction proceeding through a radical pair intermediate is used to enhance ^{19}F nuclear magnetisation in 3-fluorotyrosine by more than an order of magnitude with a corresponding increase in the amplitudes of ^{19}F–^{1}H cross-relaxation and cross-correlation effects. The reactions employed are cyclic and leave the sample chemically unchanged. The potential for enhancing the sensitivity of heteronuclear NOEs in ^{19}F-labelled proteins is discussed.

Keywords: NMR; CIDNP; NOE; Fluorine; Amino acid

1. Introduction

Chemically induced dynamic nuclear polarisation (CIDNP) is the name given to the non-equilibrium nuclear spin state populations produced in chemical reactions that proceed through radical pair intermediates. Detected as enhanced absorptive or emissive signals in the NMR spectra of the reaction products, CIDNP has been exploited for the last 30 years to characterise transient free radicals and their reaction mechanisms [1,2]. In certain cases, CIDNP also offers the possibility of large improvements in NMR sensitivity. The principal application of this photo-CIDNP technique, as devised by Kaptein [3], has been to proteins in which the aromatic amino acid residues histidine, tryptophan, and tyrosine can be polarized using flavins or other aza-aromatics as photosensitisers [4,5]. The key feature of the method is that only solvent-accessible histidine, tryptophan, and tyrosine residues can undergo the radical pair reactions that result in nuclear polarisation. Photo-CIDNP has thus been used to probe the surface structure of proteins, both in native and partially folded states, and their interactions with molecules that modify the accessibility of the reactive side chains [4–8].

Photo-CIDNP experiments on proteins using an argon ion laser as the light source and flavin mononucleotide (FMN) as the photosensitizer routinely exhibit ^{1}H NMR signal enhancements of up to 10-fold. Heavier spin-1/2 nuclei (^{13}C, ^{15}N, and ^{19}F) often show larger polarisations [6,9]. It is demonstrated below that a 20- to 40-fold ^{19}F hyperpolarisation can be created and sustained for several seconds in a photo-CIDNP experiment on 3-fluorotyrosine.

We explore the possibility of using ^{19}F photo-CIDNP as a source of strong long-range ^{19}F–^{1}H heteronuclear Overhauser effects (NOEs). We describe measurements to characterise the ^{19}F–^{1}H dipole–dipole (DD) cross-relaxation and DD-CSA (chemical shift anisotropy) cross-correlation effects associated with ^{19}F photo-CIDNP in 3-fluorotyrosine (Fig. 1), chosen as a test compound because of its simple ^{19}F–^{1}H spin system and the relative ease with which fluorotyrosine-labelled proteins can be produced [10].

2. Theory

The production of CIDNP by continuous low-power illumination of an NMR sample in a strong magnetic field can be described by adding constant magnetisation-source terms to the equation of motion of the density

* Corresponding author. Fax: +44-1865-275410.
E-mail address: peter.hore@chem.ox.ac.uk (P.J. Hore).

1090-7807/$ - see front matter © 2004 Elsevier Inc. All rights reserved.
doi:10.1016/j.jmr.2004.01.011

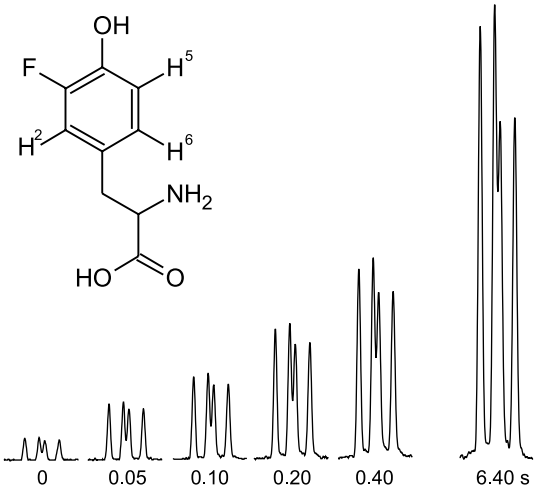

Fig. 1. ^{19}F NMR spectra of 3-fluorotyrosine as a function of laser irradiation time. The spectrum labelled "0" is the conventional NMR spectrum. Irradiation was performed prior to the 90° pulse in a single-scan pulse-acquire experiment.

operator of the spin system in the absence of the photochemical reaction (i.e., in the dark) [11]:

$$\frac{\mathrm{d}\hat{\rho}}{\mathrm{d}t} = \left(\frac{\mathrm{d}\hat{\rho}}{\mathrm{d}t}\right)_{\mathrm{dark}} + \sum_i p_i \hat{I}_z^i, \tag{1}$$

where $\hat{I}_z^i$ is the z-magnetisation operator for the ith nucleus and p_i is the corresponding photo-CIDNP magnetisation pumping rate, which can be either positive or negative. The CIDNP source terms are non-stochastic and time-independent, so they appear unchanged in the magnetisation mode evolution equations obtained after treating the spin system in the Redfield relaxation matrix formalism [12]. CIDNP multiplet effects [1,2], if present, can be introduced by adding similar source terms for the longitudinal multi-spin orders.

Although a rigorous analysis of the longitudinal cross-relaxation of the fluorine and the H(2) proton in 3-fluorotyrosine (see Fig. 1 for numbering scheme) should strictly include all three protons in the aromatic ring, and possibly also the βCH_2 and αCH protons, it will be shown below that the experimental data are fully described by a simpler relaxation model that includes the interaction of the anisotropically shielded ^{19}F nucleus with the adjacent H(2) as an AX spin system and neglects the contributions of the remote protons.

The longitudinal relaxation equations for a weakly coupled two spin–spin system when one spin has an anisotropic chemical shift tensor have been obtained by Goldman [13]. After introduction of the CIDNP source term, these expressions become:

$$\frac{\mathrm{d}}{\mathrm{d}t}\begin{bmatrix} 1 \\ H_z \\ F_z \\ 2H_zF_z \end{bmatrix} = -\begin{bmatrix} 0 & 0 & 0 & 0 \\ -p_{\mathrm{H}} & \rho_{\mathrm{HH}} & \sigma_{\mathrm{HF}} & 0 \\ -p_{\mathrm{F}} & \sigma_{\mathrm{HF}} & \rho_{\mathrm{FF}} & \delta_{\mathrm{F,HF}} \\ 0 & 0 & \delta_{\mathrm{F,HF}} & \rho_{\mathrm{HFHF}} \end{bmatrix}\begin{bmatrix} 1 \\ \Delta H_z \\ \Delta F_z \\ 2H_zF_z \end{bmatrix}, \tag{2}$$

where ΔH_z and ΔF_z are the deviations of the ^{1}H and ^{19}F z-magnetisations from equilibrium ($\Delta H_z = H_z - H_{z0}$, and similarly for ΔF_z) and $2H_zF_z$ is the longitudinal ^{1}H–^{19}F two-spin order. Although the self-relaxation parameters ρ_{HH}, ρ_{FF}, and ρ_{HFHF} contain contributions from relaxation mechanisms other than the DD and CSA mechanisms, the dipolar cross-relaxation rate σ_{HF} and the rate of accumulation of longitudinal two-spin order $\delta_{\mathrm{F,HF}}$ arise in this system solely from dipolar interactions and DD-CSA cross-correlation. These parameters may be written as [13,14]:

$$\begin{aligned}\sigma_{\mathrm{HF}} &= \frac{1}{10}\left(\frac{\mu_0}{4\pi}\right)^2 \frac{\gamma_{\mathrm{H}}^2\gamma_{\mathrm{F}}^2\hbar^2\tau_{\mathrm{c}}}{r_{\mathrm{HF}}^6} \\ &\quad\left(\frac{6}{1+(\omega_{\mathrm{F}}+\omega_{\mathrm{H}})^2\tau_{\mathrm{c}}^2} - \frac{1}{1+(\omega_{\mathrm{F}}-\omega_{\mathrm{H}})^2\tau_{\mathrm{c}}^2}\right), \\ \delta_{\mathrm{F,HF}} &= \frac{2}{5}\frac{\mu_0}{4\pi}\frac{\gamma_{\mathrm{F}}^2\gamma_{\mathrm{H}}\hbar B_0}{r_{\mathrm{HF}}^3}\frac{\tau_{\mathrm{c}}}{1+\omega_{\mathrm{F}}^2\tau_{\mathrm{c}}^2}\Delta\sigma_{\mathrm{F}}^g,\end{aligned} \tag{3}$$

where r_{HF} is the proton–fluorine distance, τ_{c} is the rotational correlation time, and $\Delta\sigma_{\mathrm{F}}^g$ denotes

$$\begin{aligned}\Delta\sigma_{\mathrm{F}}^g = &\frac{1}{2}\sigma_{XX}(3\cos^2\theta_{X,\mathrm{HF}} - 1) + \frac{1}{2}\sigma_{YY}(3\cos^2\theta_{Y,\mathrm{HF}} - 1) \\ &+ \frac{1}{2}\sigma_{ZZ}(3\cos^2\theta_{Z,\mathrm{HF}} - 1),\end{aligned} \tag{4}$$

in which σ_{XX}, σ_{YY}, σ_{ZZ} are the principal elements of the anisotropic part of the chemical shift tensor and $\theta_{X,\mathrm{HF}}$, $\theta_{Y,\mathrm{HF}}$, $\theta_{Z,\mathrm{HF}}$ are the angles between the corresponding principal axes and the H–F vector. Although it is often assumed that ^{19}F shielding tensors in fluorine-substituted benzenes are axially symmetric, calculations reveal a significant rhombicity [15]. Eq. (4), rather than the expression for an axial tensor [14], is therefore preferred.

In the extreme narrowing limit and taking $B_0 = 14.1\,\mathrm{T}$ (600 MHz proton frequency), one obtains the following expressions for the cross-relaxation rates:

$$\begin{aligned}\sigma_{\mathrm{HF}}/\mathrm{Hz} &= 2.52\times10^{11}\frac{\tau_{\mathrm{c}}/\mathrm{s}}{(r_{\mathrm{HF}}/\mathrm{\AA})^6}, \\ \delta_{\mathrm{F,HF}}/\mathrm{Hz} &= 1.01\times10^{9}\frac{\tau_{\mathrm{c}}/\mathrm{s}\,\Delta\sigma_{\mathrm{F}}^g/\mathrm{ppm}}{(r_{\mathrm{HF}}/\mathrm{\AA})^3}.\end{aligned} \tag{5}$$

The integrated form of Eq. (2) can be directly fitted to experimental data to obtain values of the parameters. Once both σ_{HF} and $\delta_{\mathrm{F,HF}}$ are known, simple arithmetic gives $\Delta\sigma_{\mathrm{F}}^g$ and τ_{c}. Care must be taken to ensure that the appropriate multipliers are introduced to account for

the difference in the equilibrium polarisations of protons and fluorine if both are normalised to unity.

3. Experimental methods

^{1}H and ^{19}F photo-CIDNP spectra were recorded on a 600 MHz (14.1 T) NMR spectrometer equipped with a 5 mm ^{19}F–{^{1}H} probe. The light source was a Spectrophysics Stabilite 2016-05 argon ion laser, operating in multi-line mode at 5 W output power, principally at 488 and 514 nm. A mechanical shutter controlled by the spectrometer was employed to produce light pulses of 0.05–6.40 s duration. The light was brought into the 5 mm sample tube from above via a 1 mm diameter optical fibre (Newport F-MBE), positioned inside a coaxial insert (Wilmad WGS 5BL) whose tip was 2 mm above the top of the NMR coil [16]. After shimming, this arrangement has no adverse effect on the NMR resolution or line shape and requires no modification to the NMR probe [17]. An airtight sample re-injection system was employed to counteract depletion of the photosensitizer [17], such that there was negligible photoreduction for up to 12 s total irradiation time.

A D_2O solution containing 4 mM 3-fluoro-DL-tyrosine (Lancaster) and 0.2 mM FMN (Sigma Aldrich) at pH 5.0 (uncorrected for deuterium isotope effect), purged with argon for 20 min, was used in all experiments. During each experiment the sample was irradiated for a prescribed time and, after a variable relaxation delay, subjected to a 90° pulse on either ^{1}H or ^{19}F followed by immediate acquisition of the free induction decay. No paramagnetic broadening was detected in any of the 3-fluorotyrosine spectra, consistent with the low steady state concentration of radicals produced during the irradiation periods and their rapid recombination when the light is extinguished.

Table 1
Calculated isotropic hyperfine coupling constants for the 3-fluorotyrosyl radical compared to the computed and experimental [21] HFCs of the tyrosyl radical

Nucleus	Tyrosyl		3-Fluorotyrosyl
	Experimental (HFC/mT)[a]	Computed (HFC/mT)	Computed (HFC/mT)
H(2)	0.15	0.26	0.28
H(3)/F(3)	0.65	−0.68	1.57
H(5)	0.65	−0.68	−0.62
H(6)	0.15	0.26	0.20

[a] The signs of the experimental values were not determined.

After application of a shifted gaussian window function, zero-filling and Fourier transformation, the spectra were integrated using mixed lorentzian-gaussian line fitting. The magnitudes of the F_z, $2H_z^{(2)}F_z$, $2H_z^{(5)}F_z$, and $4H_z^{(2)}H_z^{(5)}F_z$ magnetisation modes at the end of the relaxation delay were calculated from the integrals of individual lines in the ^{19}F multiplet. Eq. (2) was solved using a 4th-order adaptive grid Runge–Kutta method with 10^{-10} relative error on each integration step. Minimisation of the weighted least squares error functional was performed using the Nelder–Mead simplex method. A Monte-Carlo method was employed to estimate errors in the fitting parameters. Libraries supplied with the Matlab 6.0 software package were used for all these computations.

Computation of in vacuo equilibrium geometry and hyperfine coupling constants were performed using the GAMESS program [18] at the DFT U-B3LYP 6-311G**/EPR-III level. The in vacuo ^{19}F magnetic shielding tensor was estimated using Gaussian98 [19] at the GIAO HF 6-311++G(2d, 2p) level using the 3-fluorotyrosine geometry obtained from a separate U-B3LYP 6-311G** GAMESS calculation. The relatively inexpensive Hartree–Fock-based computation of the shielding tensor was used because previous studies had

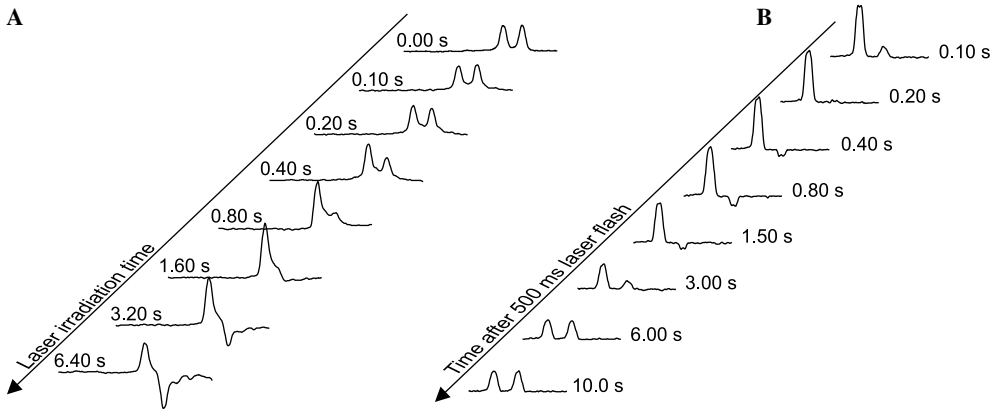

Fig. 2. The H(2) resonance taken from 600 MHz ^{1}H photo-CIDNP NMR spectra of 3-fluorotyrosine as a function of: (A) laser irradiation time and (B) the time after a 0.5 s laser flash. The gradual deterioration in the spectral resolution in set (A) is due to non-uniform sample heating by the laser.

revealed no obvious advantage of MP2 or DFT based methods for the ^{19}F nuclei of the molecules in question [20]. The calculated hyperfine couplings for the neutral radicals derived from tyrosine and 3-fluorotyrosine by abstraction of hydrogen from the phenolic OH group are given in Table 1 together with the experimental values for the tyrosyl radical [21].

4. Results

Figs. 1–3 show the changes in the ^{19}F and ^{1}H NMR spectra and polarisations of 3-fluorotyrosine produced by laser irradiation. Under continuous irradiation the fluorine CIDNP magnetisation pumping rate is $p_F = +34\,s^{-1}$ (Figs. 1 and 3A, left hand panel), i.e., the initial build-up rate of the F_z mode corresponds to the accumulation of 34-fold ^{19}F hyperpolarisation per second. The CIDNP magnetisation pumping rate for the adjacent H(2) proton is $p_H = +1.3\ s^{-1}$, hence the initial slow rise (Fig. 3A, right hand panel). After four seconds of irradiation, the ^{19}F z-magnetisation reaches a steady state, in which the CIDNP magnetisation pumping is balanced by relaxation, corresponding to 24 times the equilibrium magnetisation (Fig. 3A, left hand panel). Under continuous laser irradiation the ^{19}F magnetisation stays at this level. Under identical conditions, the polarisation of H(3) in tyrosine itself has a much smaller pumping rate, $p_H \approx -5\,s^{-1}$.

Increasing the laser output power from 5 to 25 W gives up to 40-fold ^{19}F hyperpolarisation in the 3-fluorotyrosine-FMN system. Higher polarisation is difficult to obtain due to sample heating by the intense laser light.

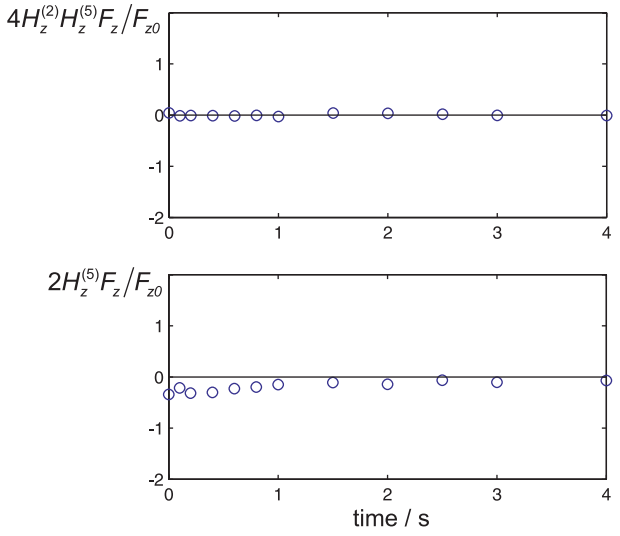

Fig. 4. The amplitudes of two fluorine longitudinal multi-spin orders as a function of time after a 0.5 s laser flash.

As shown by the unequal multiplet component intensities in Figs. 1 and 2, longitudinal two-spin order, $2H_z^{(2)}F_z$, accumulates as a result of cross-correlation between the F-H(2) DD interaction and the fluorine CSA (Eq. (2)). In the case of continuous irradiation (Fig. 3A, centre panel) the amplitude of $2H_z^{(2)}F_z$ after several seconds of irradiation attains a steady state value of $2H_z^{(2)}F_z/F_{z0} = -2.0$. Such a magnitude of ^{1}H–^{19}F two-spin order is impossible to generate using

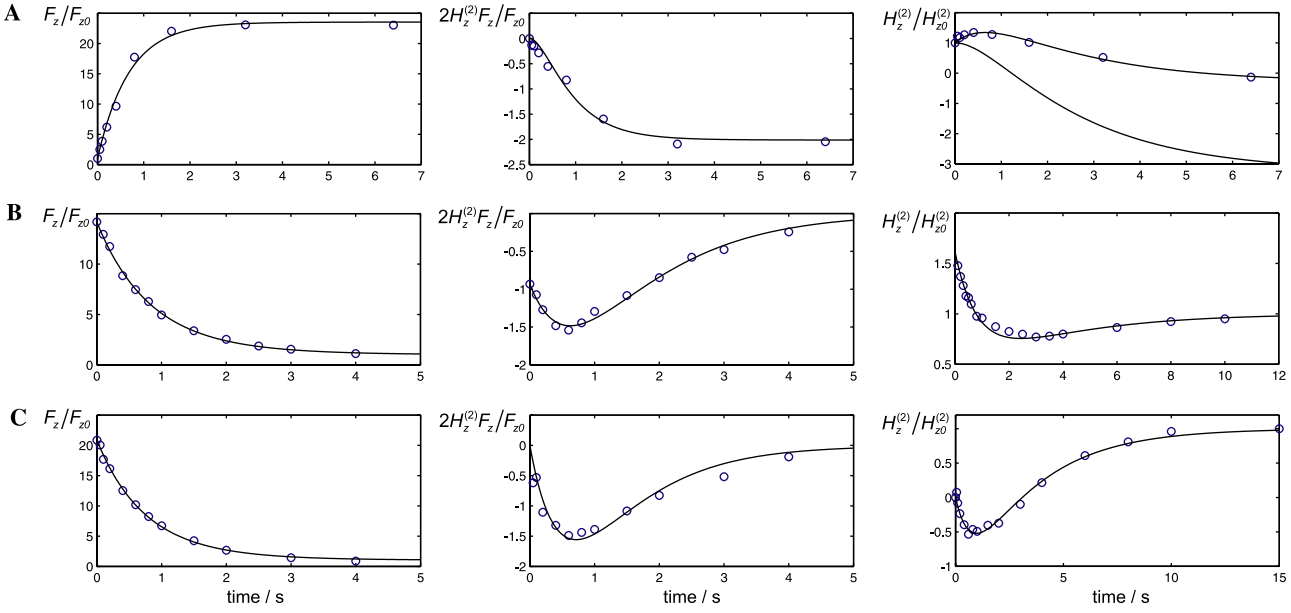

Fig. 3. The time dependence of three longitudinal magnetisations in the F–H(2) spin system in 3-fluorotyrosine. (A) With continuous laser irradiation. The lower curve in the right hand panel is the polarisation computed in the absence of ^{1}H CIDNP. (B) As a function of mixing time after a 0.5 s laser flash. (C) As a function of mixing time after a 1.0 s laser flash with ^{1}H decoupling during irradiation. The solid lines are the results of fitting Eq. (2) to the data.

Table 2
Experimental DD and DD-CSA cross-relaxation rates, rotational correlation times, and ^{19}F geometrically weighted shielding anisotropy for the F–H(2) spin system of 3-fluorotyrosine

Experiment	$\delta_{F,HF}$ (s^{-1})	σ_{HF} (s^{-1})	τ_c (ps)	$\Delta\sigma_F^g$ (ppm)
Continuous irradiation	0.27 ± 0.07	0.088 ± 0.003	108 ± 4	44 ± 11
After 0.5 s irradiation	0.24 ± 0.04	0.087 ± 0.012	106 ± 15	39 ± 8
After 1.0 s irradiation with ^{1}H decoupling	0.30 ± 0.05	0.094 ± 0.008	115 ± 10	45 ± 8

traditional NMR methods. The maximum value of $2H_zF_z/F_{z0}$ obtained by Dorai and Kumar [22] for similar molecules by inversion of the ^{19}F equilibrium magnetisation was about 0.15.

The amplitudes of the longitudinal multi-spin magnetisation orders of fluorine with other protons, such as $2H_z^{(5)}F_z$ and $4H_z^{(2)}H_z^{(5)}F_z$ as determined from the relative integrals of the ^{19}F multiplet components, are barely above the noise level of the integration (Fig. 4), justifying the approximation (see above) that these modes do not contribute significantly to the longitudinal cross-relaxation within the F–H(2) spin system. As can be seen from Fig. 3, the experimental data for 3-fluorotyrosine are very satisfactorily described using this approximation.

The time dependence of the H(2) z-magnetisation is a result of competition between direct CIDNP pumping and ^{19}F–^{1}H dipolar cross-relaxation (Fig. 3A, right hand panel). The CIDNP of H(2) in tyrosine and 3-fluorotyrosine is weakly absorptive, and causes the H_z polarisation to rise initially to about 150% of the equilibrium polarisation. However, the negative NOE from the highly polarised ^{19}F nucleus gradually overwhelms the ^{1}H CIDNP: after about six seconds of irradiation the observed ^{1}H polarisation is pushed below zero, corresponding to a NOE of around −100%, resulting from competition between ^{1}H CIDNP pumping and the ^{19}F–^{1}H NOE. In complex molecules (e.g., a ^{19}F-labelled protein) most protons have no CIDNP of their own. Solving Eq. (2) with p_H set to zero leads to an actual NOE magnitude of around −400% after six seconds of irradiation (Fig. 3A, right hand panel).

The ^{19}F–^{1}H spin system shows similar behaviour in dynamic CIDNP NOE experiments. The three panels in Fig. 3B show the magnetisation evolution after a 500 ms laser flash. Because the ^{19}F CIDNP enhancement after 500 ms irradiation is only about 15-fold and decays quickly, the cross-relaxation and cross-correlation effects are weaker, but still very pronounced. In particular, it can be seen that the $2H_z^{(2)}F_z/F_{z0}$ two-spin order first grows to an amplitude of −1.5 and then decays to zero. The longitudinal ^{1}H magnetisation $H_z^{(2)}$ first loses the CIDNP that accumulated during the irradiation, briefly dips about 25% below its equilibrium value as a result of the ^{19}F–^{1}H NOE, and gradually relaxes to equilibrium. Solving Eq. (2) using $p_H = 0$ gives a NOE of −55%.

As mentioned above, the ^{19}F–^{1}H NOE is considerably more pronounced when the proton has no counteracting CIDNP of its own. This can be demonstrated in the case of 3-fluorotyrosine by destroying the ^{1}H CIDNP by decoupling the protons during the laser flash. Fig. 3C shows the evolution of the magnetisation modes after a 1.0 s laser flash, with ^{1}H decoupling. Once the decoupler is switched off (at $t = 0$), the $H_z^{(2)}$ magnetisation abruptly goes negative as a result of the ^{19}F–^{1}H NOE, reaching a value of $H_z^{(2)}/H_{z0} = -0.5$, which is above the maximum theoretical NOE for conventional NMR and exceeds the magnitudes of ^{19}F–^{1}H NOEs usually observed in such systems by a factor of five.

The DD and DD-CSA cross-relaxation rates measured for the F–H(2) spin system are presented in Table 2. The values of the correlation time τ_c and the ^{19}F CSA were calculated using a F–H(2) distance of 2.60 Å, obtained by ab initio computation in vacuo. Within experimental error, the three sets of measurements give the same values for τ_c and $\Delta\sigma_F^g$. The values of $\Delta\sigma_F^g$ agree well with those reported for similar molecules by Dorai and Kumar [22].

The orientation of the computed ^{19}F nuclear shielding tensor is shown schematically in Fig. 5. The computation yields the absolute chemical shielding tensor with the following eigenvalues: $\sigma_{11} = 326 \pm 10$ ppm, $\sigma_{22} = 357 \pm 10$ ppm, $\sigma_{33} = 436 \pm 10$ ppm. The error estimates are based on the discrepancies between calculated and experimental shielding tensor components in a study by Dios and Oldfield [15]. The most shielded component σ_{33} was found to be perpendicular to the benzene ring plane, and the least shielded component

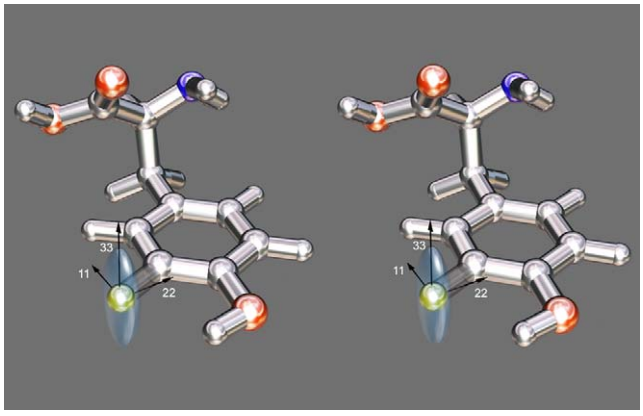

Fig. 5. Stereo view of the orientation of the fluorine magnetic shielding tensor in 3-fluorotyrosine in vacuum as computed using GIAO HF 6-311++G(2d, 2p) theory on a DFT B3LYP 6-311G** optimized geometry.

σ_{11} to be at a 25° angle to the direction of the F–H(2) vector. The resulting computed geometrically weighted anisotropy, $\Delta\sigma^g_F$, was 62 ± 30 ppm.

5. Discussion

The relatively large ^{19}F CIDNP build-up rate reported above ($+34\,s^{-1}$) compared to the corresponding proton in tyrosine ($-5\,s^{-1}$) is at least partially due to the different magnetic properties of the intermediate radicals. The ^{19}F hyperfine coupling constant computed for the 3-fluorotyrosyl radical is +1.57 mT (Table 1) as opposed to −0.65 mT for the corresponding proton in the tyrosyl radical [21]. For non-viscous solutions and in a strong magnetic field, the geminate CIDNP effect of a particular nucleus is proportional to its hyperfine coupling constant in the intermediate radical [11]. Larger hyperfine interactions also lead to faster nuclear spin–lattice relaxation in the radical and hence less cancellation of recombination and escape polarisation in the cyclic reaction scheme [5]. Although a full explanation of this effect will require experiments with microsecond time-resolution [23,24], its consequences may nonetheless be put to good use.

Fig. 3A shows that 20-fold ^{19}F hyperpolarisation can be sustained for at least seven seconds by continuous laser irradiation with no damage (or indeed any change at all) to the 3-fluorotyrosine sample. If the same holds true in a complex molecular system, such as a fluorine-labelled protein, this implies that long-distance dipolar energy transfer could occur, either directly or mediated by intervening protons.

The measured dipolar cross-relaxation rates and NOE magnitudes allow one to speculate about CIDNP-induced ^{19}F–^{1}H NOEs when 3-fluorotyrosine is incorporated into a larger molecule. Assuming that the destination atom has no CIDNP of its own (which would normally be the case) and taking the detectable NOE enhancement to be about 1%, one can make a rough estimate that an NOE effect that reaches a magnitude of 400% at 2.60 Å distance would be still detectable at distances of up to about $2.60(400)^{1/6} = 7$ Å.

A consideration of the dependence of the polarisation transfer rates on the rotational correlation time (Fig. 6) provides another argument in favour of chemically pumped ^{19}F–^{1}H NOEs. The isotropic correlation time for 3-fluorotyrosine is about 10^{-10} s, with the result that both σ_{HF} and $\delta_{F,HF}$ are comparable and relatively small. For a (~25 kDa) protein with τ_c of about 20 ns, however, the DD cross-relaxation rate σ_{HF} would be approximately 30 times larger, while the cross-correlation rate is barely changed. This does not necessarily imply a 30-fold increase the CIDNP NOE, because longitudinal self-relaxation will also be faster in the more slowly tumbling molecule, but it certainly means that the drain

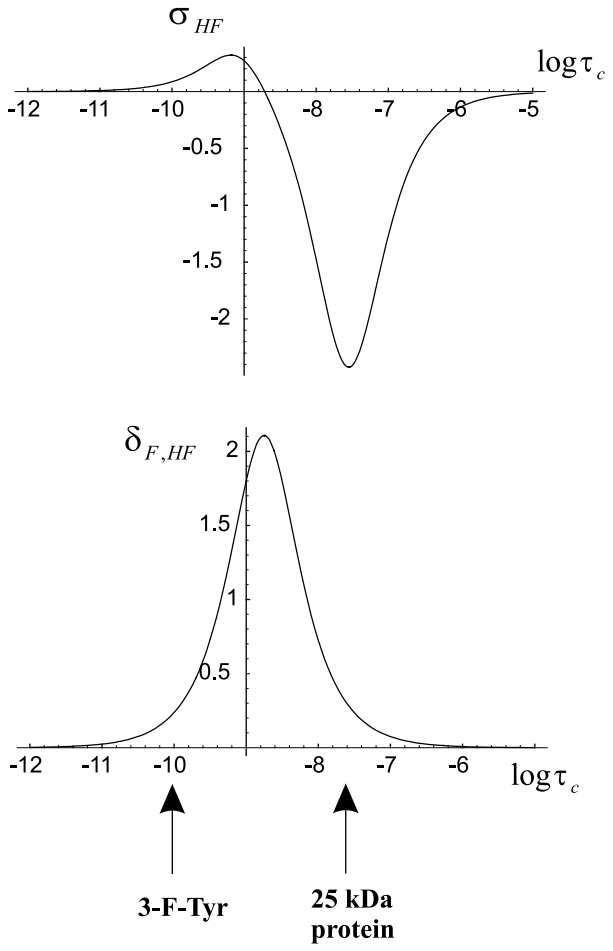

Fig. 6. Dependence of the DD cross-relaxation rate σ_{HF} and the rate of accumulation of longitudinal multi-spin order $\delta_{F,HF}$ on the rotational correlation time. Calculated from Eq. (3) using $r_{HF} = 2.60$ Å and $\Delta\sigma^g_F = 40$ ppm.

of fluorine magnetisation into longitudinal multi-spin orders will be reduced.

In most one- and multi-dimensional experiments, using CIDNP as a source of strong nuclear polarisation amounts simply to adding photosensitizer to the sample and inserting a laser flash at the start of the pulse sequence [6], accompanied, if necessary, by simultaneous decoupling to remove undesired direct CIDNP effects. For experiments requiring a large number of scans, photosensitizer depletion can be countered by employing a sample re-injection device [17].

We suggest that the phenomenon explored here could be referred to as the Chemically Amplified Nuclear Overhauser Effect, CANOE.

Acknowledgments

This work was supported by BBSRC, INTAS (project 01-2126) and the EU (RTD project HPRI-1999-CT-50006). We are indebted to Maša Čemažar, Charles

Lyon and Kiminori Maeda for preliminary experiments, to Nick Soffe, Jonathan Boyd and Pete Biggs for expert technical assistance, and to Iain Day, Ken Hun Mok, and Alexandra Yurkovskaya for helpful discussions. IK thanks the Scatcherd European Foundation and the Hill Foundation for financial support.

References

[1] L.T. Muus, P.W. Atkins, K.A. McLauchlan, J.B. Pedersen (Eds.), Chemically Induced Magnetic Polarisation, D. Reidel, Dordrecht, 1977.
[2] M. Goez, Photochemically induced dynamic nuclear polarization, Adv. Photochem. 23 (1997) 63–163.
[3] R. Kaptein, Photo-CIDNP studies of proteins, Biol. Magn. Res. 4 (1982) 145–191.
[4] R. Kaptein, K. Dijkstra, K. Nicolay, Laser photo-CIDNP as a surface probe for proteins in solution, Nature 274 (1978) 293–294.
[5] P.J. Hore, R.W. Broadhurst, Photo-CIDNP of biopolymers, Prog. NMR Spectrosc. 25 (1993) 345–402.
[6] C.E. Lyon, J.A. Jones, C. Redfield, C.M. Dobson, P.J. Hore, Two-dimensional ^{15}N–^{1}H photo-CIDNP as a surface probe of native and partially structured proteins, J. Am. Chem. Soc. 121 (1999) 6505–6506.
[7] C.E. Lyon, E.-S. Suh, C.M. Dobson, P.J. Hore, Probing the exposure of tyrosine and tryptophan residues in partially folded proteins and folding intermediates by CIDNP pulse-labelling, J. Am. Chem. Soc. 124 (2002) 13018–13024.
[8] K.H. Mok, T. Nagashima, I.J. Day, J.A. Jones, C.J.V. Jones, C.M. Dobson, P.J. Hore, Rapid sample-mixing technique for transient NMR and photo-CIDNP spectroscopy: applications to real-time protein folding, J. Am. Chem. Soc. 125 (2003) 12484–12492.
[9] B.D. Sykes, J.H. Weiner, Biosynthesis and NMR characterisation of fluoroamino acid containing proteins, in: J.S. Cohen (Ed.), Magnetic Resonance in Biology, vol. 1, Wiley, New York, 1980, pp. 171–196.
[10] B.D. Sykes, H.I. Weingarten, M.J. Schlesinger, Fluorotyrosine alkaline phosphatase from *Escherichia coli*: preparation, properties, and fluorine-19 nuclear magnetic resonance spectrum, Proc. Natl. Acad. Sci. USA 71 (1974) 469–473.
[11] P.J. Hore, M.R. Egmond, H.T. Edzes, R. Kaptein, Cross-relaxation effects in the photo-CIDNP spectra of amino acids and proteins, J. Magn. Res. 49 (1982) 122–150.
[12] A.G. Redfield, The theory of relaxation processes, Adv. Magn. Res. 1 (1965) 1–32.
[13] M. Goldman, Interference effects in the relaxation of a pair of unlike spin-1/2 nuclei, J. Magn. Res. 60 (1984) 437–452.
[14] A. Kumar, R.C.R. Grace, P.K. Madhu, Cross-correlations in NMR, Prog. NMR Spectrosc. 37 (2000) 191–319.
[15] A.C. Dios, E. Oldfield, Evaluating ^{19}F chemical shielding in fluorobenzenes: implications for chemical shifts in proteins, J. Am. Chem. Soc. 116 (1994) 7453–7454.
[16] J.E. Scheffler, C.E. Cottrell, L.J. Berliner, An inexpensive, versatile sample illuminator for photo-CIDNP on any NMR spectrometer, J. Magn. Res. 63 (1985) 199–201.
[17] K. Maeda, C.E. Lyon, J.J. Lopez, M. Čemažar, C.M. Dobson, P.J. Hore, Improved photo-CIDNP methods for studying protein structure and folding, J. Biomol. NMR 16 (2000) 235–244.
[18] M.W. Schmidt, K.K. Baldridge, J.A. Boatz, S.T. Elbert, M.S. Gordon, J.H. Jensen, S. Koseki, N. Matsunaga, K.A. Nguyen, S.J. Su, T.L. Windus, M. Dupuis, J.A. Montgomery, General atomic and molecular electronic structure system, J. Comput. Chem. 14 (1993) 1347–1363.
[19] M.J. Frisch, G.W. Trucks, H.B. Schlegel, G.E. Scuseria, M.A. Robb, J.R. Cheesn, V.G. Zakrzewski, J.A. Montgomery Jr., R.E. Stratmann, J.C. Burant, S. Dapprich, J.M. Millam, A.D. Daniels, K.N. Kudin, M.C. Strain, O. Farkas, J. Tomasi, V. Barone, M. Cossi, R. Cammi, B. Mennucci, C. Pomelli, C. Adamo, S. Clifford, J. Ochterski, G.A. Petersson, P.Y. Ayala, Q. Cui, K. Morokuma, P. Salvador, J.J. Dannenberg, D.K. Malick, A.D. Rabuck, K. Raghavachari, J.B. Foresman, J. Cioslowski, J.V. Ortiz, A.G. Baboul, B.B. Stefanov, G. Liu, A. Liashenko, P. Piskorz, I. Komaromi, R. Gomperts, R.L. Martin, D.J. Fox, T. Keith, M.A. Al-Laham, C.Y. Peng, A. Nanayakkara, M. Challacombe, P.M.W. Gill, B. Johnson, W. Chen, M.W. Wong, J.L. Andres, C. Gonzalez, M. Head-Gordon, E.S. Replogle, J.A. Pople, Gaussian 98, Revision A.11.1, Gaussian, Pittsburgh PA, 2001.
[20] L.K. Sanders, E. Oldfield, Theoretical investigation of ^{19}F NMR chemical shielding tensors in fluorobenzenes, J. Phys. Chem. A 105 (2001) 8098–8104.
[21] M. Tomkiewicz, R.D. McAlpine, M. Cocivera, Photooxidation and decarboxylation of tyrosine studied by EPR and CIDNP techniques, Can J. Chem. 50 (1972) 3849–3856.
[22] K. Dorai, A. Kumar, Fluorine chemical shift tensors in substituted fluorobenzenes using cross correlations in NMR relaxation, Chem. Phys. Lett. 335 (2001) 176–182.
[23] M. Goez, Pulse techniques for CIDNP, Conc. Magn. Res. 7 (1995) 263–279.
[24] O.B. Morozova, A.V. Yurkovskaya, Yu.P. Tsentalovich, M.D.E. Forbes, P.J. Hore, R.Z. Sagdeev, Time resolved CIDNP study of electron transfer reactions in proteins and model compounds, Mol. Phys. 100 (2002) 1187–1195.